Polym. Korea, Vol. 46, No. 4, pp. 444-454 (2022)
https://doi.org/10.7317/pk.2022.46.4.444

ISSN 0379-153X(Print)
ISSN 2234-8077(Online)

Flexible Polyurethane Foam에서 화염확산에 대한 발화위치와 샘플 두께의 영향

Qi Yuan*, Chang Li***, Paul Amyotte****, Lingfeng Wang*,
Chunmiao Yuan*,**,†, Gang Li*, and Weidong Yan***
*Fire & Explosion Protection Laboratory, Northeastern University
**State Key Laboratory of Explosion Science and Technology, Beijing Institute of Technology
***Department of Civil Engineering, Shenyang Jianzhu University
****Department of Process Engineering, Applied Science, Dalhousie University
(2021년 12월 9일 접수, 2022년 3월 10일 수정, 2022년 4월 27일 채택)

Effect of Ignition Position and Sample Thickness on Flame Spread in Flexible Polyurethane Foam

Qi Yuan*, Chang Li*, Paul Amyotte****, Lingfeng Wang*,**
Chunmiao Yuan*,,†, Gang Li*, and Weidong Yan*****

**Fire & Explosion Protection Laboratory, Northeastern University, Liaoning, Shenyang 110819, China*
***State Key Laboratory of Explosion Science and Technology, Beijing Institute of Technology, Beijing 100081, China*
****Department of Civil Engineering, Shenyang Jianzhu University, Liaoning, Shenyang 110168, China*
*****Department of Process Engineering, Applied Science, Dalhousie University, Halifax NS, B3H 4R2, Canada*
(Received December 9, 2021; Revised March 10, 2022; Accepted April 27, 2022)

Abstract: Fire behavior of flexible polyurethane foam (FPUF) at different sample thicknesses and ignition positioning was investigated. Effects on flame height, mass loss rate and other parameters were tested, and the flame propagation mechanism was analyzed. A method for predicting equivalent combustion diameter (D) values of the dynamic change of liquid pool at different positions is proposed. Combined with data of sample mass loss rate, flame height can be predicted. Based on a transition state model, a method for predicting the fire risk of FPUF in late stage combustion by calculating the generation time of polyols is proposed. With edge ignition, FPUF burning produces an inclined surface during the combustion process which enhances the length of the preheating zone by means of heat conduction and heat radiation. Flame spread rate (FSV) in FPUF with edge ignition was greater than with center point ignition.

Keywords: flexible polyurethane foam, sample thickness, ignition position, fire behavior, equivalent combustion diameter.

Introduction

Flexible polyurethane foam (FPUF) is the dominant combustible constituent of building insulation materials,[1,2] upholstered furniture,[3] and cleaning tools among other products. In 2011, a particularly serious accident caused by the burning polyurethane foam insulation occurred in the Jing An District of Shanghai, China. Once ignited, fire may spread rapidly, releasing CO_2 and HCN (hydrogen cyanide). People exposed to the fumes of burning polyurethane foam often have difficulty escaping, presenting significant challenges for fire fighting personnel.[4] While the fire hazard of large-scale FPUF is concerned, it seems that small-scale (approximately 10-20 cm) kitchen cleaning products containing FPUF should also be considered dangerous.

Factors affecting flame spread in solid polymer materials, mainly include the thickness,[5] width[4] and inclination angle[6-9] of the sample, along with atmospheric pressure,[6-11] and radiation input from external sources.[4,11] Thickness greatly influenced combustion characteristics of polymer materials, increasing pool fire length and average flame side area.[12] For PMMA, increased fuel thickness increased flame size, which in turn increased the angle between the flame and the unburned fuel,

†To whom correspondence should be addressed.
yuanchunmiao@mail.neu.edu.cn, ORCID 0000-0002-3024-8053

with convection the primary factor controlling heat transfer in thermal thin materials.[13] For rubber latex foam with bottom ventilation, flame spread rate (FSV) in thermally thin natural latex foam was 2.93 mm/s, which was greater than with thermally thick latex foam.[14] Based on thermal transfer theory, Delichtsios *et al*.[15] analyzed the influence of material thickness on flame propagation.

In flame spread experiments, the ignition position is often fixed at the center or edge.[8,16] The influence of the ignition position during combustion is often ignored. In real life, due to unexpected accidents or arson fire, materials can be ignited from any point.[17] The effect of different ignition positions on flames in the premixed hydrogen/air in a finite-sized enclosed tube has been determined.[18] In fires longitudinal spread, a polymer object ignited in the center of the lower edge initially generated more heat than did the lower right edge.[17] This has not been observed, however, in some horizontal flame spread experiments with polymers. FSV in latex foam ignited along an edge was higher than with center point ignition.[19,20] It appears that ignition positioning may be the dominant influence on the development of flame spread with various mechanisms. In 2019, Flecknoe-Brown and Hees[21] proposed that the ignition position significantly influences numerically simulated FSV in FPUF However, the effect of ignition position on other combustion characteristics in FPUF has not been investigated. Quantitative assessment of the impact of ignition conditions should be considered indispensable in fire safety design.[17]

The research was designed to further determine the influence of ignition position on the fire risk of small-size (10×10 cm) FPUF with different thickness by using a horizontal experimental platform to determine relevant fire risk parameters. Three thicknesses (2, 4, and 6 cm) and two ignition position (center or edge) were selected as test conditions. These results can also provide data supporting the fire risk assessment of small-sized FPUF cleaning tools and the improvement of related standards.

Experimental

Experimental Procedure and Apparatus. The surface temperature profile, flame spread rate and mass loss are important parameters in response to the fire hazard of the material. The experimental test apparatus and procedure of fire hazard parameters were referenced to the standard GB/T 25353-2010 (Figure 1(a)).[22] The experimental platform were used to determine changes in flame spread using a method modified from Huang *et al*.[23,24] and Yan *et al*.[25] In order to exclude the influence of environmental parameters on the experimental results, each group of experiments was completed in a laboratory with controlled temperature and humidity. The environmental parameters are shown in Table 1.

The fire hazard testing apparatus is usually included systems for ventilation, flame spread testing, data acquisition, and data processing (Figure 1(b)). Flue gas generated during combustion was collected by a ventilation hood and then discharged through a pipe. The fire test system consisted of a sample holder and insulation board along with an ignition resource. Test samples were placed in the 0.3×0.3×0.3 m steel sample holder with a 0.4×0.4 m heat-insulating bottom board. The board was placed between the sample holder and the electronic balance to reduce the influence of heat on the top surface of the electronic balance. Another 0.3×0.3 m heat insulation board was positioned above the sample holder, thereby cutting off ventilation to the bottom of the experimental sample. The sample holder and two heat insulation boards rested on the electronic balance (range 2 kg, accuracy 0.01 g).

The data acquisition system consisted of K-type armored thermocouples, one thermos hygrometer and two CCD cameras. The temperature measurement range of the thermos hygrometer is -10-50 ºC, the humidity measurement range is 5%RH-98%RH, and the sampling frequency is 1 time/s. K-type armored thermocouples, 0.5 mm diameter, T1, T2, and T3

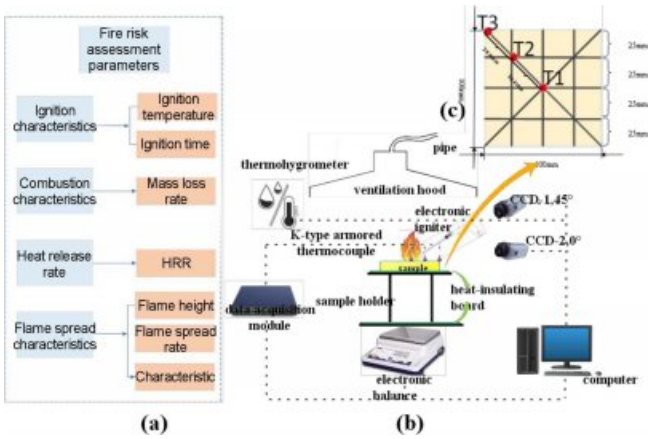

Figure 1. Experimental platform of flame spread: (a) fire hazard test parameters; (b) experiment setup; (c) FPUF.

Table 1. Environmental Parameters

Region	Ambient atmospheric pressure (KPa)	Ambient temperature (K)	Humidity (%)
123.4E 41.8N	100	293	35

were connected to a multi-channel data acquisition module (DAM-3138) and a data transfer cable (DAM-2121N, Altai Technology, China) to record sample surface temperatures during combustion. The armored portion of the thermocouple was 0.3 m long, while the bare wire length was 1.5 m. Temperature measurement range was -20 to 1300 ºC. The three thermocouples were positioned 35.4 mm apart (Figure 1(c)).

CCD-1 and CCD-2 cameras, with a resolution of 25 fps and positioned at 0 and 45º angles off the sample surface, were used to determine changes in flame height and horizontal flame spread across the sample surface. Specifically, 25 images per second were captured from the CCD-1 and CCD-2 cameras. Actual flame height data was processed by a MATLAB procedure with image recognition and processing functionality. After binarizing images taken by the CCD camera, momentary flame height was obtained by setting scale parameters. Finally, temperature, mass loss, and video data were transmitted to the computer.

To analyze the sample combustion mechanism, thermal degradation behavior was measured by a German NETZSCH thermogravimetric analyzer (TGA). Samples with 2.01±0.005 mg were used under air environment for pyrolysis. The TG curve was obtained under a heating rate of 10 ºC/min with gas flow of 20 mL/min.

Materials. FPUF with a size of 100×100×20 mm was supplied by Jiangsu Jintu Home Furnishing Co., Ltd, which produced by pre-polymerization method (Table 2). The main materials of FPUF are polyol, diisocyanate, foam stabilizer (polyether siloxane), chain extender (1,3-Dihydroxypropane) and blowing agent (non-flame retardant), etc. The surface of the FPUF was marked with straight lines every 25 mm to facilitate determination of the flame front position (Figure 1(b)). Samples were oven-dried at 40 ºC for 12 hours prior to experimentation. Each experiment was replicated three times.

The ignition source was an electronic igniter using liquid n-butane as fuel. In this experiment, with reference to the standard GB/T 25353-2010,[22] a device that removes the igniter from the ignition position is installed to ensure the same contact time between the igniter and the samples surface of each group. Preliminary testing ensured that the sample could be ignited and then removed when the ignition source was activated and held at the ignition point for 2 s. Fuel consumption of the electronic igniter was 0.4 mL for each experiment. The ignition design of each group of experiments was the same except for the position of the ignition point so as to eliminate the influence of different initial ignition energy of the combustion process.

Table 2. Introduction of FPUF

Density (kg/m^3)	Pore size (μm)	Pyrolysis temperature (°C)	Thermal conductivity ($W \cdot m \cdot K^{-1}$)	Combustion heat (J/kg)
25	50	190	0.035	25

Results and Discussion

Molecular Properties of FPUF. The zero-dimensional microscopic TG analysis reflects the thermal stability and components of the FPUF. The TG curve of FPUF shows that mass loss was occurring in three stages. The temperature in the first stage was 0-190 ºC, during which the water in the sample evaporated, and mass loss was 8.58%. The temperature in the second stage was 190-408 ºC. During this period, the sample decomposed rapidly and a large amount of harmful gas was generated by mass loss at 79.6%. During the third stage, samples burned out gradually at 408-665 ºC, and mass loss was about 10.8%. The TG curves of FPUF and two other common polymer materials (expandable polystyrene board (EPS) and extruded polystyrene (XPS)) are compared in Figure 2.[26] The peak mass loss was observed in the EPS at 377.4-413.3 ºC. The mass loss of XPS at 228-298 ºC was 7.1%, while mass loss at 342-456 ºC was 87.6%. Ignition point and pyrolysis temperature of the FPUF were lower than those of the other two materials. FPUF began decomposing dramatically at 190 ºC, while EPS and XPS began their dramatic decomposition at 377 and 342 ºC, respectively. FPUF may have a higher fire risk than EPS and XPS. The activation energy of FPUF is lower than that of polystyrene, so it burns more readily.[27]

The FPUF decomposition process shows pyrolysis reaction rates and combustion of volatiles are interdependent (Figure 3). The primary reactions associated with FPUF burning are

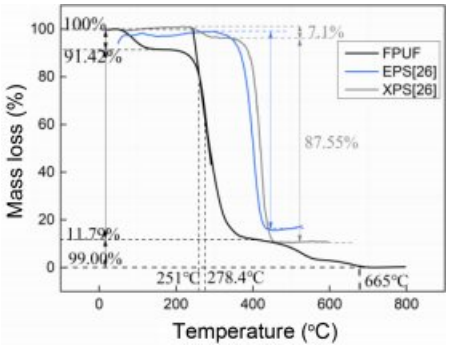

Figure 2. TG-DSC testing of FPUF.

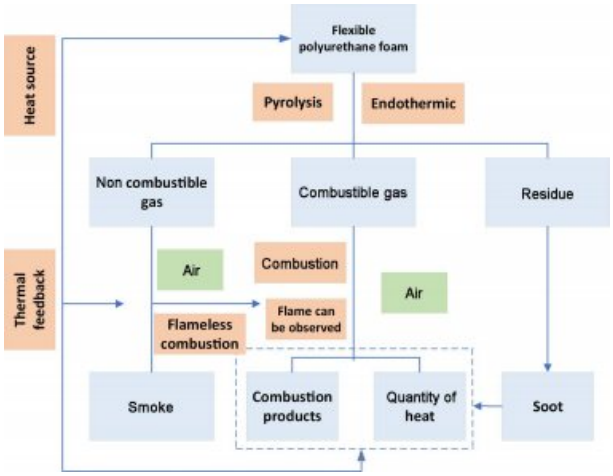

Figure 3. FPUF decomposition process.

shown in[28]:

Oxidation reaction:

$$FPUF + O_2 = polyols + OH \quad (1)$$

$$polyols + O_2 = char + OH + H_2CO + CO + CO_2 \quad (2)$$

$$char + O_2 = residue + OH + H_2CO + CO + CO_2 \quad (3)$$

Pyrolysis reaction:

$$FPUF = polyols + TDI \quad (4)$$

$$polyols = H_2O + CH_4 + OH + H_2CO \quad (5)$$

Where TDI is toluene diisocyanate. The oxidation reaction is limited by the oxygen consumption of the flame on the fuel surface. Oxidation reactions usually play a role in the early and decaying stages of a fire, but not in the PPUF pyrolysis process during combustion.[29] FPUF pyrolysis causes cracking in TDI and polyols. Subsequently, a liquid pool and toluene diisocyanate (combustible gas) were observed.[6,28]

Fire Behavior. Flame spread in samples with different thicknesses and ignition positioning was determined by the CCD camera. Sample thickness had little effect on flame spread, which developed in three stages, namely initial growth, stable combustion, and decay. During stable combustion, large flame pulsation was observed and was attributed to the upward movement of combustible gas released during combustion, causing vortex flow in the combustion chamber. This phenomenon is similar to the self-sustaining oscillating flame of a pool fire and is driven by buoyancy caused by the temperature gradient between the boundary layer and the surrounding fluid. Eventually a diffuse flame form.[30,31] In the case of pool fire combustion, flame pulsation frequency is governed by the Grashof number (*Gr*), which characterizes the parameters of buoyancy and viscous forces in convective heat transfer, as calculated by eq. (6).[30]

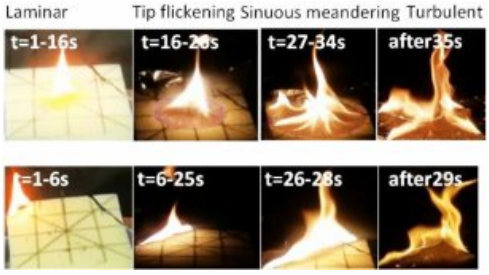

Figure 4. Effect of Gr number on the flame structure in FPUF with sample thickness of 2 cm, P=1 atm and T=293 K.

$$Gr = \frac{(P/RT_\infty)^2 g l^3}{\mu^2} \quad (6)$$

Where P is standard atmospheric pressure, R is the gas constant, T_∞ is ambient temperature, g is acceleration due to gravity, μ is the dynamic viscosity of the air, and l is the length of the liquid pool during combustion time t of the experiment.

Flame structure during combustion of FPUF can be divided into four stages (laminar flame, Tip flickering flame, sinuous meandering flame and turbulent flame) using calculated *Gr* values.[30] Figure 4 shows the influence of *Gr* number on flame shape in FPUF for a sample thickness of 2 cm. Given the central point ignition, the laminar flame transformed into tip flickering at 11 s, and further transformed into sinuous meandering at about 16 s. When the flame front spread to the sample edges, the flame transformed into turbulent flame. With edge ignition, the flame morphology still underwent these four changes, but the duration of each morphological stage was different. This is because the position of the flame front differed between center and edge positioning at each moment. Eventually the characteristic length of the formed 'liquid pool' began to vary.

Mass Loss. Sample mass gradually decreased during combustion (Figure 5(a)-(c)). For samples having the same thickness, peak mass loss rate with central point ignition was greater but more residues were observed on the heat insulating board of the sample holder. With center point ignition, combustion residues of samples with thicknesses of 2, 4, and 6 cm were 18.3, 13.2, and 13.8%, respectively. Combustion residues of samples with thicknesses of 2, 4, and 6 cm with edge ignition were 13.2, 11.9, and 12.8%, respectively. As the sample thickness increased, residue percentage decreased slightly. This may be due to the fact that FPUF is a thermoset material.[27,32] After the char is pyrolyzed by FPUF, it drips onto the insu-

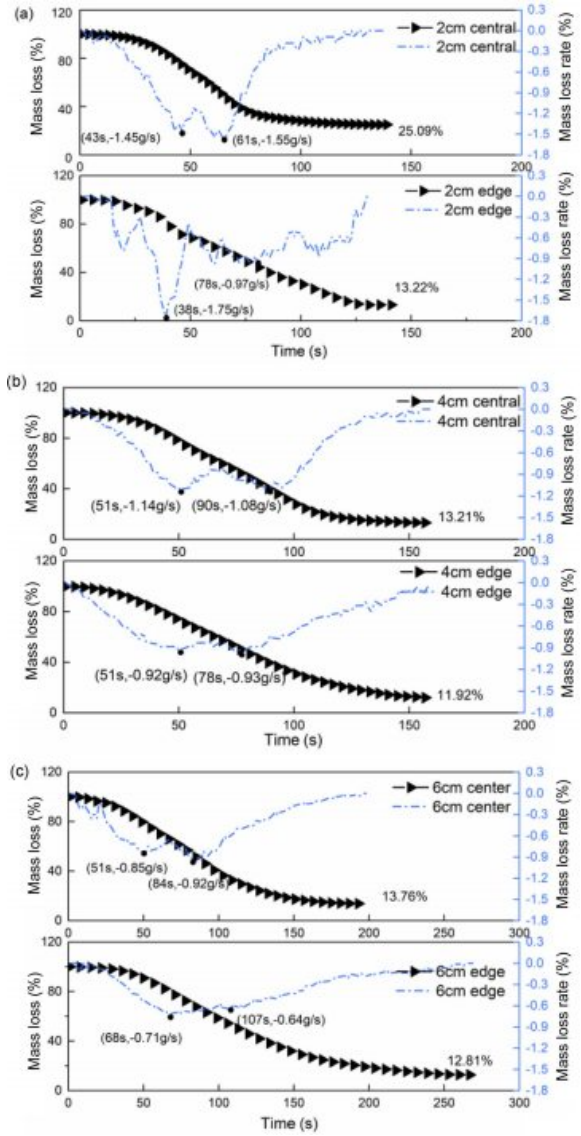

Figure 5. FPUF mass loss with different ignition positions: (a) 2 cm; (b) 4 cm; (c) 6 cm.

lation board and continues to burn. The longer the sample is burned, the more fully the bottom 'liquid pool' burns. When the ignition position is moved from center point to edge, the residue mass decreases. This may be due to the fact that unburned char is heated by a larger flame area with edge ignition, thus causing the char to burn more completely.

Mckeen[28] proposed a three stage model by including a transitional stage where FPUF was converted to polyol. This transition is represented by a transitional layer composed of FPUF and polyol (Figure 6(a)). The model is proposed based on the variation of HRR (heat release rate) values with time. There is a linear relationship between HRR values and mass loss rates.

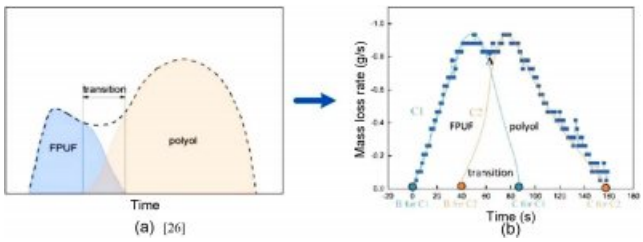

Figure 6. Method for calculating the duration of sample transition state: (a) the transition state model proposed by Mckeen[28]; (b) calculation method of the transition state duration based on mass loss.

Therefore, in combination with Machen's model, the mass loss rate is used to predict the duration of the three stages (Figure 6(b)). Taking trough 'A' of the demarcation point, the quality loss rate was divided into two curves named C1 and C2. The two fitted curves C1 and C2 can be derived. According to these derived curves the intersection points B and C of the curve y=0 and C1 or C2 can be solved during the combustion time.

According to Table 3, the duration of the first stage of FPUF samples with thicknesses of 2, 4, and 6 cm under conditions of central ignition was 14, 15, and 27 s, respectively. The duration of the second phase (transition state) was 35, 78, and 39 s, respectively. The duration of polyol was 31, 54, and 105 s, respectively. Polyols form a flowing liquid pool which may pose a higher fire risk. In other words, FPUF with a thickness of 6 cm seems more dangerous in the late stage of combustion. As sample thickness increased, duration of the transition state was nonlinear. The duration of the first stage of FPUF samples with the thicknesses of 2, 4, and 6 cm under conditions of edge ignition was 31, 48, and 38 s. Duration of the first stage with edge ignition was longer than with center ignition. Duration of the transition stage was 8, 28, and 73 s. The transition state of 2 and 4 cm samples with edge ignition was much shorter than that with center ignition. During the last stage, duration was

Table 3. Fitting Curve Equation

Sample	Fitting curve	Ignition position			
		Center		Edge	
		B/s	C/s	B/s	C/s
2 cm	C1	10.0	59.5	14.2	53.8
	C2	24.2	91.0	45.6	130.2
4 cm	C1	1.0	94.0	4	78
	C2	16	158	51	150
6 cm	C1	1	87.2	6.5	117
	C2	48	192	44	265

about 76, 72, and 148 s. The decomposition time of the polyol at this stage was longer with edge ignition than with center ignition, which further explains why the mass of the sample residue with center ignition was more than that with edge ignition.

In addition, the duration of the liquid pool with edge ignition was longer than that with central ignition, and thus edge ignition may more readily ignite other surrounding materials. The flame spread rate is used to judge the fire risk of a material in its initial stage of combustion.[23] Given the melting properties of FPUF, it seems that its fire risk in the late stage of combustion can be determined by calculating the generation time and duration of polyols using this method.

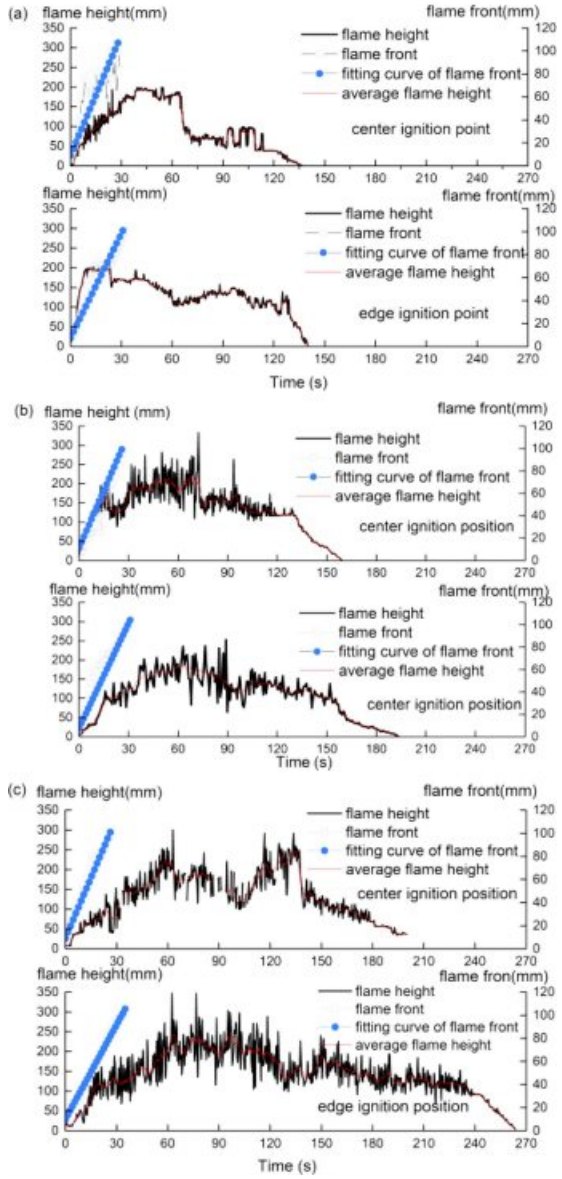

Figure 7. Flame height and flame front position in FPUF at different sample thicknesses and ignition positioning: (a) 2 cm; (b) 4 cm; (c) 6 cm.

Flame Height. Flame height is an indicator of the intensity of sample burning, and is closely related to the surrounding radiant heat.[33] Figure 7(a-c) shows the change in flame height and flame front position when 2, 4, and 6 cm samples were ignited from the edge or from a center point. Flame height fluctuation was similar to that reported previously.[23] After sample ignition, flame height gradually increased, followed by smooth pulsation within a certain range. As sample burning neared completion, flame height dropped. As FPUF continued to burn, large amounts of molten FPUF accumulated in the chassis, giving rise to a second peak in flame height. Flame height then decreased as sample burning neared completion. The dual peaks in the mass loss rate curves discussed in section mass loss may be explained as follows.

During stable combustion, flame height of 2, 4, and 6 cm samples with central point ignition was 54-193, 106-203, and 139-231 mm, respectively. Corresponding flame height with edge ignition was 99-176, 117-256, and 136-266 mm, respectively. Maximum flame height with thicknesses of 2, 4, and 6 cm and with central point ignition was 194, 161, and 222 mm, respectively. Corresponding maximum flame height with edge ignition was 197, 192, and 239 mm, respectively. In addition, as sample thickness increased, maximum flame height and average flame height increased. With the greater thickness, flame height in FPUF decreased initially and then increased. For equally thick samples, maximum and average flame height with edge ignition were larger than with center point ignition, suggesting a higher fire risk with edge ignition. However, increasing sample thickness did not change the effect of ignition positioning on the hazard.

Flame height was determined using a customized MATLAB program. Flame height could also be calculated as follows[34]:

$$\frac{H}{D} = 3.7Q^{*} - 1.02 \tag{7}$$

Where H is flame height and D is equivalent combustion diameter, both in mm. D is calculated as follows:

$$D = 2\sqrt{\frac{WL}{\pi}} \tag{8}$$

where W and L are width and length of samples, respectively, in mm.

Q^{*} is the dimensionless heat release rate, in W, which can be determined as follows:

$$Q^* = \frac{\dot{Q}}{\rho_0 C_{pa} T_0 g^{0.5} D^{\frac{5}{2}}} \quad (9)$$

where ρ_0 is ambient air density, in kg/m^3, T_0 is ambient temperature, in K, g is acceleration due to gravity, in N/kg, and Q is the total heat release rate, in W, which can be obtained as follows:

$$\dot{Q} = \text{MLR} \times Q \quad (10)$$

where MLR is mass loss rate, in g/s. Q is the calorific value. The heat of combustion of polyurethane is 24-26 J/kg.[28]

A portion of the surface of the FPUF appeared similar to a liquid pool. But unlike a typical burning pool fire, the diameter of the 'liquid pool' changed dynamically from the beginning to the end of the flame spread. D of the liquid pool during the entire process of flame spread was calculated by eq. (8), which underestimates flame height at the beginning and end. Therefore, at the beginning and end of flame spread with central ignition position, the equivalent combustion diameter, D, of the liquid pool was calculated as follows:

$$D_{\text{center}} = 2Ff \quad (11)$$

Ff is flame front position, in mm, which can be obtained using a MATLAB program.

The equivalent combustion diameter of the sample with edge ignition position can be calculated as follows:

$$D_{\text{edge}} = 2\sqrt{\frac{\cos\alpha Ff \times \sin\alpha Ff}{\pi}} \quad (12)$$

Where α is the angle in degrees between the position of the flame front and the edge of the sample.

Thus, eq. (10), (11), and (12) provide a possibility for predicting flame height of the entire combustion stage with central or edge ignition, while eq. (7) predicts variable liquid pool diameter (D). The experimental value for flame height along with its theoretical value calculated by eq. (8) compare well in Figure 8(a-c). This predictive method for FPUF flame height in pool fires may be used whenever FPUF materials were melting properties.

Flame Spread Rate and Area Expansion Rate of the Burning Zone. Horizontal direction flame front of FPUF advance increases linearly with time during the initial stage (Figure 7). Average flame spread rate of selected other polymers (rubber latex foam[14] and XPS[12]) is given in Figure 9(a) for comparison with FPUF. FSV in samples with a given ignition positioning vary sample thickness, reaching a maximum

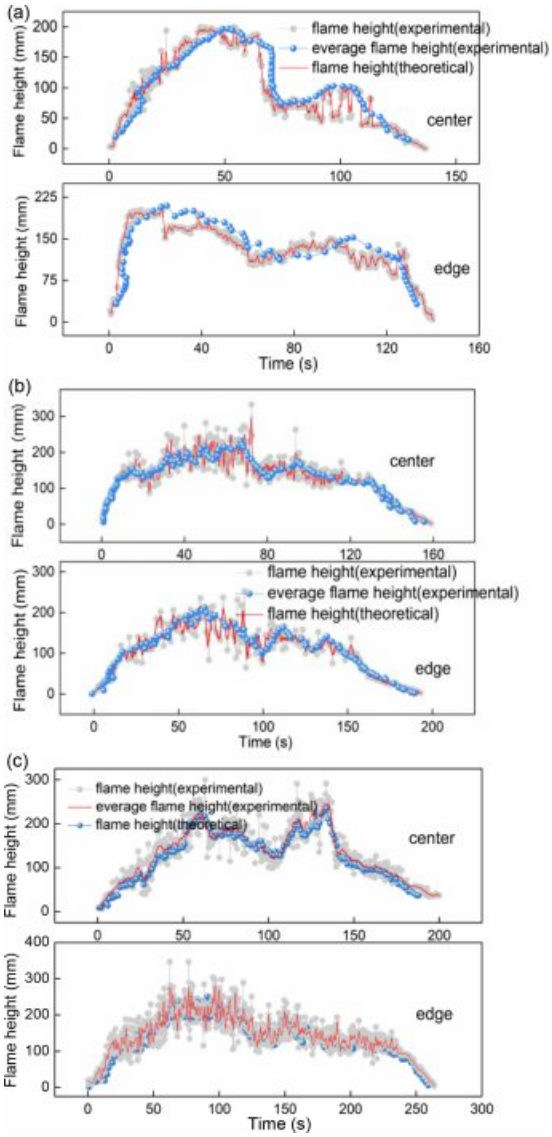

Figure 8. Theoretical calculation of flame height: (a) 2 cm; (b) 4 cm; (c) 6 cm.

at 4 cm. A similar trend is reported for XPS and rubber latex foam.[12,14] As the sample thickness increased to 6 cm, fire spread rate decreased. This may have been due to both chemical and thermal effects giving rise to different combustion energies.[35] With thickness increases, the heat transfer pattern of the sample undergoes a transition from thermally thin to thermally thick control. In order to more accurately describe the multi-dimensional flame spread process of the samples, the expansion area of burning zone is mentioned (Figure 9(b)). Average area expansion of the burning zone with thickness of 2, 4, and 6 cm and central point ignition was 2.76, 3.39, and 2.91 cm^2/s, respectively. Corresponding average area expansion of burning zone with edge ignition were 4.96, 5.36, and

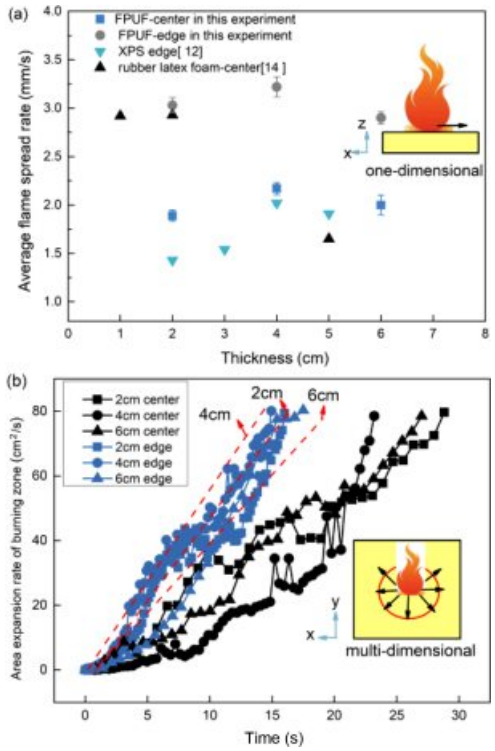

Figure 9. Average FSV and area expansion: (a) average FSV; (b) area expansion of burning zone.

4.59 cm^2/s, respectively. Thus, the average area expansion rate of the burning zone with edge ignition was 79.7% (2 cm), 58.1% (4 cm), and 57.7% (6 cm) higher than that with the central point ignition. The reason that the area expansion of burning zone shows the same variety as the flame spread rate is that the flame front (circular) of this material tends to be uniform in all directions. In addition, differences in sample flame spread behavior due to different ignition locations were noted.

Temperature Profile. Temperature changes at the sample surface and temperature gradient changes at the ignition position are shown in Figure 10(a-c). With central point ignition, flame spread towards T3, T2, and T1, causing temperature to increase sharply. Values for dT/dt_{max} of 2, 4, and 6 cm samples with central point ignition were 80.0, 105.5, and 79.6 K/s, respectively. For edge ignition, corresponding dT/dt_{max} values were 129.5, 127.0, and 140.3 K/s, respectively. At a given sample thickness, dT/dt_{max}, values for edge ignition were higher than those with central point ignition. This was due to the relatively large area of contact with air for samples with edge ignition. At a given ignition positioning, dT/dt_{max} values first increased and then decreased as sample thickness increased, as is typically observed with surface fire spread rate.

Since samples with thicknesses of 4 and 6 cm melted faster

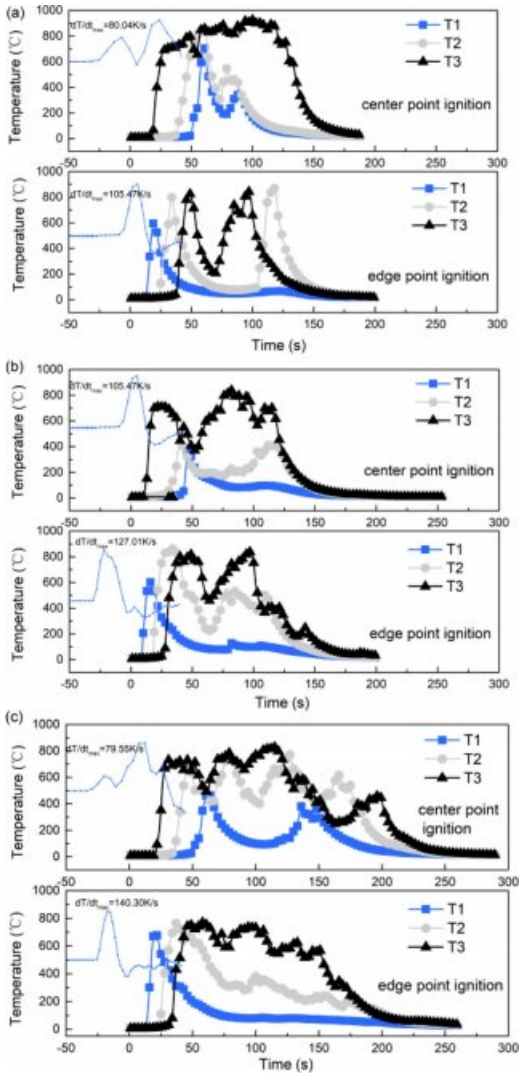

Figure 10. Temperature profiles in FPUF at different sample thicknesses and ignition positioning: (a) 2 cm; (b) 4 cm; (c) 6 cm.

than the 2 cm sample during combustion, the upper surface temperature dropped more rapidly. Temperature increased dramatically during flame spread. The time from T2 to T3 for flame spread of samples with central point ignition was shorter than that for T1 to T2, which indicates that horizontal flame spread in central point ignition samples accelerated. This effect was not significant with edge ignition, however. Two peaks were observed in the temperature change in edge ignition samples. After the T1 position was ignited, flames spread horizontally and downward. Subsidence of the burning sample layer separated the thermocouple from the sample, causing monitored temperature to decrease. When the sample melted and dropped, a large amount of molten FPUF was present on the surface of the insulated sample holder, causing flame height

to increase again. This behavior is also reflected in Figure 7.

Further Discussion. As seen in section flame spread, FSV in samples with edge ignition was higher than that with central point ignition. In Figure 11, q_f is heat radiation, and $q_{k,p}$ indicates heat conduction. The horizontal arrow points in the direction of heat conduction. The vertical arrow indicates that thermal radiation decreases as distance from the fire source increases. During sample combustion, a flame front formed an angle, θ, with the sample surface. After the sample center was ignited, the flame front spread outward concentrically. As combustion began, the middle of the sample began to sink where the burnout zone was located. After flames spread to the sample surface, burning continued. Because the sample edge had a large area of contact with air, it burned more rapidly. Consequently, the center of the sample became convex during the latter stage of combustion (Figure 11(a)). In this situation, the value θ was >90º. When samples were ignited from the edge, flames spread in a diagonal direction, with the flame front forming an arc. The sample edges burned rapidly and were consumed more rapidly. The contact angle between the flame and the sample surface decreased to a θ value of <90º, resulting in an inclined surface (Figure 11(b)). The inclination angle of the sample surface slope is denoted as β. Tu *et al.*,[6,8] Zhou *et al.*,[36] and Ma *et al.*[9] reported that the increase in inclination angle leads to complex changes in flame propagation rate due to the conversion between different thermal feedback mechanisms.

With 2, 4, and 6 cm thickness and edge ignition, θ values were >90º with center ignition, but θ fluctuated around 60-90º with edge ignition. Only when the flame front spread to the entire upper sample surface did θ values approach or exceed 90º (Figure 12). In section flame spread we noted that FSV with edge ignition was higher than that with center ignition. This may be because, with a decreased θ, the effect of radiation and convection heat transfer was enhanced, and the length of the preheating zone was also increased, which in turn led to an increase in FSV.

The relationship between sinβ and time and the instanta-

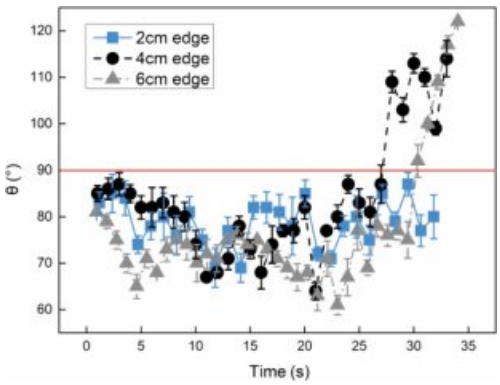

Figure 12. Variation law of FSV with θ.

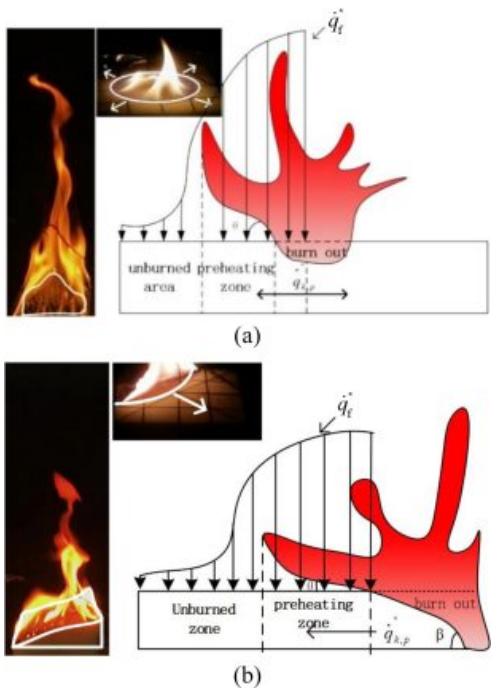

Figure 11. Flame spread mechanism: (a) center point ignition; (b) edge ignition.

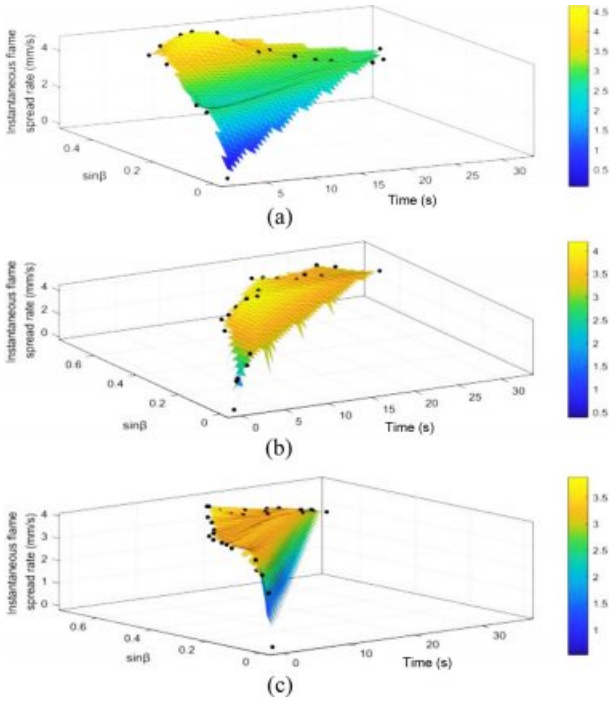

Figure 13. Variation law of instantaneous FSV with sinβ and time: (a) 2 cm; (b) 4 cm; (c) 6 cm.

neous FSV in horizontal fire spreading with edge ignition is given in Figure 13(a-c). The value of sinβ increased initially and then decreased with time. $q_{k,p}$ (heat conduction) increased with the increase of β. β values and instantaneous FSV with edge ignition first increased and then fluctuated within a certain range. For 2-cm-thick PFUF, sinβ increased from 0 to 0.48 (29º), and then fluctuated in the range of 0.36-0.57. In this case, maximum instantaneous FSV was 4.6 mm/s at about 9 s. For 4 cm-thick PFUF, sinβ increased from 0 to 0.64 (40º), and then fluctuated from 0.47-0.73 (43º). Instantaneous FSV reached a maximum of 4.7 mm/s at about 14 s under these conditions. For 6 cm-thick PFUF, sinβ increased from 0 to 0.68, and then fluctuated in the range of 0.62-0.89, with an instantaneous fire spread rate maximizing at 3.9 mm/s at approximately 17 s. The increase in sample thickness may increase the slope angle β, thereby enhancing heat transfer. This provides further confirmation that FSV in edge ignited samples has been always higher than that with central ignition. This is similar to the principle governing pool fires, namely that flame diffusion rate is higher on an inclined surface, causing sample thickness to decrease rapidly. It should be noted that sample ignition from the edge is the reason for the formation of this slope. In addition, combustion consumption also increases with an increase in combustion surface area.[34] However, increasing sample thickness did not change the effect of ignition positioning on hazard.

Conclusions

1) Based on the transition state model, a method is proposed for predicting the fire hazard of FPUF with melting characteristics in the later stage of combustion by calculating the generation time of polyols.

2) A method is proposed for estimating dynamic change of D values (diameter of the liquid pool) during FPUF combustion with either edge or center point ignition. Flame height is predicted by a combination of D and mass loss rate. Predicted values show good agreement with experimental results. The prediction method for liquid flame height can be extended to FPUF and similar materials.

3) Unlike samples with central point ignition, samples with edge ignition formed a slope during combustion, meaning that the contact angle, θ, between flame front and the sample surface decreased. The slope increased the length of the preheating zone, and flame spread more rapidly during the early stage of combustion, showing a higher ignition risk. However, increasing sample thickness did not change the effect of ignition positioning on the hazard.

Acknowledgment(s): The authors gratefully acknowledge financial support from the National Natural Science Foundation of China (Nos. 51974189, 51874070), Fundamental Research Funds for the Central Universities (N2101003, N2101042), Young researcher project of the Education Department of Liaoning Province (No. lnqn202006), Innovative talents program of Liaoning Province (No. XLYC2007089), Liaoning Provincial Natural Science Foundation of China (19-ZD-0668, 2020-KF-13-01), and Shenyang Science and Technology Program (20-206-4-23). This research was also supported by the opening project of State Key Laboratory of Explosion Science and Technology (Beijing Institute of Technology, KFJJ22-19M) and State Key Laboratory of Strata Intelligent Control and Green Mining Co-founded by Shandong Province and the Ministry of Science and Technology (SICGM202205). The author Chang Li acknowledges financial support from the China Scholarship Council (No. 202008210136) during her visit to Dalhousie University.

Conflict of Interest: The authors declare that there is no conflict of interest.

References

1. Ma, X.; Tu, R.; Cheng, X. D.; Zhu, S. G.; Sun, Q.; Fang, T. Y. Sub-Atmospheric Pressure Coupled with Width Effect on Downward Flame Spread over Energy Conservation Material Polyurethane Foam. *J. Therm. Sci.* **2020**, 29, 115-121.
2. Huang, X. J.; Wang, C. J.; Gao, J. D.; Zhou, Z. J.; Tang, G.; Wang, C. Research on Two Sides Horizontal Flame Spread Over Rigid Polyurethane with Different Flame Retardants. *J. Therm. Anal. Calorim* **2021**, 146.
3. Wang, H. S. Study on Combustion and Smoke Production Properties of Typical Upholstered Seat Materials. Ph.D. Dissertation, University of Science and Technology of China, He Fei, China, 2017.
4. Ma, X.; Tu, R.; Zhao, Y.; Xie, Q. Study on Downward Flame Spread Behavior of Flexible Polyurethane Board in External Heat Flux. *J. Thermoplast. Compos.* **2015**, 28, 1693-1707.
5. Lefebvre, J.; Bastin, B.; Bras, M. L.; Duquesne, S.; Ritter, C.; Paleja, R.; Poutch, F. Flame Spread of Flexible Polyurethane Foam: Comprehensive Study. *Polym. Test.* **2004**, 23, 281-290.
6. Tu, R.; Ma, X.; Zeng, Y.; Zhou, X. J.; Zhang, Q. X. Influences of Sub-Atmospheric Pressure on Upward Flame Spread over Flexible Polyurethane Foam Board with Multiple Inclinations. *App. Sci.* **2020**, 10, 7117.
7. Zhou, Y.; Bu, R. W.; Yi, L.; Sun, J. H. Heat Transfer Mechanism of Concurrent Flame Spread Over Rigid Polyurethane Foam: Effect of Ambient Pressure and Inclined Angle. *Int. J. Therm. Sci*. **2020**, 155, 106403.
8. Tu, R.; Ma, X.; Zeng, Y.; Zhou, X. J.; He, L.; Fang, T. Y.; Fang,

J. Coupling Effects of Pressure and Inclination on Downward Flame Spread Over Flexible Polyurethane Foam Board. *Build. Environ* **2019**, 164, 106339.
9. Ma, X.; Tu, R.; Ding, C.; Zeng, Y.; Wang, Y.; Fang, T. Y. Thermal and Fire Risk Analysis of Low Pressure on Building Energy Conservation Material Flexible Polyurethane with Various Inclined Facade Constructions. *Constr. Build. Mater.* **2018**, 167, 449-456.
10. Zhou, Y.; Xiao, H. H.; Sun, J. H.; Zhang, X. N.; Yan, W. G.; Huang, X. J. Experimental Study of Horizontal Flame Spread Over Rigid Polyurethane Foam on a Plateau: Effects of Sample Width and Ambient Pressure. *Fire Mater.* **2015**, 39, 127-138.
11. Zhou, Y.; Xiao, H. H.; Yan, W. G.; An, W.; Jiang, L.; Sun, J. H. Horizontal Flame Spread Characteristics of Rigid Polyurethane and Molded Polystyrene Foams Under Externally Applied Radiation at Two Different Altitudes. *Fire Technol*. **2015**, 51, 1195-1216.
12. Huang, X.; Zhang, Y.; Ji, J.; Yin, Y.; Sun, J. H. Thickness Effect on Flame Spread Characteristics of Extruded Polystyrene in Lhasa and Hefei Environments. *J. Comb. Sci. & Tech*. **2011**, 17, 527.
13. Jiang, L.; Miller, C. H.; Gollner, M. J.; Sun, J. H. Sample Width and Thickness Effects on Horizontal Flame Spread Over a Thin PMMA Surface. *P. Combust. Inst.* **2016**, 36, 2987-2994.
14. Yuan, Q.; Huang, D. M.; Hu, Y. W.; Shen, L. M.; Shi, L; Zhang, M. Z. Comparison of Fire Behaviors of Thermally Thin and Thick Rubber Latex Foam under Bottom Ventilation. *Polymers* **2019**, 11, 88.
15. Delichatsios, M. Effects of Material Thickness on Ignition Times and Creeping Flame Spread in the Thermal Regime: Theory, Analytical Solution and Experimental Justification. *Fire Saf. J.* **2020**, 116, 103204.
16. Huang, D. M.; Zhang, M. Z.; Guo, C. N.; Shi, L.; Lin, P. Experimental Investigations on the Effects of Bottom Ventilation on the Fire Behavior of Natural Rubber Latex Foam. *Appl. Therm. Eng.* **2018**, 133, 201-210.
17. Wang, X. G.; Cheng, X. D.; Li, L. M.; Lo, S. M.; Zhang, H. P. Effect of Ignition Condition on Typical Polymer's Melt Flow Flammability. *J. Hazard Mater*. **2011**, 190, 766-771.
18. Xiao, H. H.; Duan, Q. L.; Lin, J.; Sun, J. H. Effects of Ignition Location on Premixed Hydrogen/Air Flame Propagation in a Closed Combustion Tube. *Int. J. Hydrogen Energ.* **2014**, 39, 8557-8563.
19. Zhang, M. Z.; Huang, D. M.; Hu, Y. W.; Yuan, Q.; Xi, H. Y.; Shen, L. M.; Duan, P. Z. Effect of Ignition Position on Horizontal Flame Spread of Latex Foam. *CIESC J. (China)* **2019**, 70, 2802-2810.
20. Guo, C. N.; Huang, D. M.; Zhang, M. Z.; Zhao, Y. F. Effect of Ignition Position on Flame Spread of Natural Rubber Latex Foam. *CIESC J. (China)* **2017**, 68, 3623-3630.
21. Flecknoe-Brown, K. W.; Hees, P. V. Experimental Investigation into the Influence of Ignition Location on Flame Spread and Heat Release Rates of Polyurethane Foam Slabs. *Fire Mater*. **2021**, 45, 81-96.
22. Text Method to Determine the Flammability and Flame Propagation Characteristics of Thermal/acoustic Insulation Materials; General Administration of Quality Supervision, Inspection and Qurantine of the People's Republic of China and China National Standardization Administration Committee, 2010; GB/T 25353-2010.
23. Huang, D. M.; Chen, C.; Xu, Z. H.; Li, D.; Liang, G. H. Fire Behaviors of Two-layer Coated Latex Foam with an Extremely Thin Surface Layer Under Bottom Ventilation Conditions. *Process Saf. Environ*. **2021**, 148, 1164-1178.
24. Shen, Y. M.; Zhang, K.; Huang, D. M.; Wang, C. Y.; Chen, C.; Li, D.; Shi, L. Fire Behaviors of Multilayer Latex Foam Coated by Thin Surface Fabric under Bottom Ventilation Conditions. *Polym. Korea* **2021**, 45, 89-100.
25. Yan, W. G.; Shen, Y.; An, W. G.; Jiang, L.; Zhou, Y.; Sun, J. H. Experimental Study on the Width and Pressure Effect on the Horizontal Flame Spread of Insulation Material. *Int. J. Therm. Sci*. **2017**, 114, 114-122.
26. Jiao, L. L.; Xu, G. D.; Wang, Q. S.; Qiang, X.; Sun, J. H. Kinetics and Volatile Products of Thermal Degradation of Building Insulation Materials. *Thermochim. Acta*. **2012**, 547, 120-125.
27. Sun, J. H.; Lin, J. Thermal Analysis and Flame Spread Behavior of Building-Used Thermal Insulation Materials. *Fire Sci. & Tech.* **2015**, 45-49.
28. Mckeen, P.; Liao, Z. Y. A Three-layer Macro-scale Model for Simulating the Combustion of PPUF in CFD. *Build Simul.* **2016**, 9, 583-596.
29. Pau, D.; Fleischmann, C. M.; Spearpoint, M. J.; Li, K. Y. Thermophysical Properties of Polyurethane Foams and Their Melts. *Fire Mater.* **2014**, 38, 433-450.
30. Chen, J.; Tom, W. C.; Tang, W.; Zhang, C.; Li, C. H.; Lu, S. X. Experimental Study of the Effect of Ambient Pressure on Oscillating Behavior of Pool Fires. *Energy* **2020**, 203, 117783.
31. Fang, J.; Wang, J. W.; Guan, J. F.; Zhang, Y. M.; Wang, J. J. Momentum- and Buoyancy-driven Laminar Methane Diffusion Flame Shapes and Radiation Characteristics at Sub-atmospheric Pressures. *Fuel* **2016** 163, 295-303.
32. Huang, X. J. Study on Flame Spread Characteristics of Typical External Wall Insulation Material PS Under Different Environments. **2011**, University of Science and Technology of China, He Fei, China.
33. Ji, J.; Yuan, X. Y.; Li, K. Y.; Yang, L. Z.; Sun, J. H. A Mathematical Model for Burning Rate of n-heptane Pool Fires Under External Wind Conditions in Long Passage Connected to a Shaft. *Appl. Therm.* **2017**, 116, 91-99.
34. Zhao, J. L.; Zhu, H. Q.; Zhang, J. P.; Huang, H.; Yang, R. Experimental Study on the Spread and Burning Behaviors of Continuously Discharge Spill Fires Under Different Slopes. *J. Hazard Mater*. **2020**, 392, 122352.
35. Blasi, C. D. Influences of Sample Thickness on the Early Transient Stages of Concurrent Flame Spread and Solid Burning. *Fire Saf. J.* **1995**, 25, 287-304.
36. Zhou, Y.; Bu, R. W.; Gong, J. H.; Yan, W. G.; Fan, C. G. Experimental Investigation on Downward Flame Spread Over Rigid Polyurethane and Extruded Polystyrene Foams. *Exp. Therm. Fluid Sci*. **2018**, 92, 346-352.